

Expanding the Cathodic Potential Window of Activated Carbon Electrodes in a Lithium-Salt Containing Electrolyte

Sonia Dsoke^{*[a]}

Activated carbon is the most common material used for electrochemical double layer capacitors. With the recent development of Li-ion capacitors, activated carbon is also used in Li-salt-containing organic electrolytes. The cathodic potential of activated carbon is in general limited to 1.5 V vs. Li/Li⁺, in order to avoid the decomposition of the electrolyte, which can block the porosity and accessible area of the carbon. This work aims to investigate the unexplored region, below 1.5 V vs. Li/Li⁺ to understand how a lower limit cut-off can influence the electrochemical performance of activated carbon. Interestingly,

a very critical potential is 1.0 V. When an electrode is cycled until this limit, the performance drastically falls down. On the other side, by further expanding the lower potential limit to 0.5 V, the capacity increases, without substantially compromising the resistance and the cycling stability. At even lower potentials (i.e., 0.2 V, 0.1 V and 0.005 V) the capacity further increases, but at the cost of the cycling stability. This work opens new directions on the use of activated carbon at potentials below the standard cathodic limit of 1.5 V vs. Li/Li⁺.

1. Introduction

Activated carbon (AC) is the most common used material in electrochemical double layer capacitors (EDLCs).^[1,2] Due to its exceptionally high surface area (1500–3000 m² g⁻¹)^[3,4] AC can offer a relatively high capacitance compared to electrolytic capacitors, which are instead based on metal-type electrodes.^[5] At the state of the art, EDLCs can be engineered in aqueous or in organic-based electrolytes.^[6] Some advantages to use aqueous electrolytes are related to their environmental friendliness, their high ionic conductivity, their low price and the easy device assembly (no dry-box requirements). On the other side, despite their lower ionic conductivity and higher toxicity compared to the aqueous ones, organic electrolytes offer a higher operational potential window, which results in an enhanced energy density ($E=1/2 CV^2$). In general, the cell voltage of devices operating in organic electrolytes should be limited to 2.5–2.8 V, in order to avoid electrolyte decomposition.^[7,8] In the last years, AC was also extensively used in hybrid battery-capacitor devices, like the so-called Li-ion capacitors (LICs). LICs are in general constituted by battery-type and capacitor-type materials which are combined together in one single device.^[9–11]

In a LIC asymmetric configuration, where AC is the positive electrode, the most common battery-type negative electrodes are Li₄Ti₅O₁₂ (LTO), which operates at 1.5 V vs. Li/Li⁺ and graphite, which works at a lower potential (0.0–0.3 V vs. Li/Li⁺)

thus allowing a great increase of the energy density.^[9,10,12,13] Other materials used as negative electrodes in LiCs are graphene,^[14] hard carbon^[15] or vanadium phosphates, like Li₃V₂(PO₄)₃ (LVP),^[16] just to name a few. Other asymmetric configurations can be designed with a positive Li-insertion-type electrode (like Li₃V₂(PO₄)₃, LiMn₂O₄, LiFePO₄ etc.) and an activated carbon as negative electrode.^[17–20]

Another interesting option to design a high performance LiCs is to use the combination of two or more different active materials, having diverse energy storage mechanism, together in one electrode, thus developing a “multifunctional” electrode (or bi-material electrode).^[21–23] In the multifunctional electrode, the activated carbon enables to support high currents and the Li-intercalation material ensures enough capacity. The proper combination and ratio among the materials is crucial and can drastically affect the electrode performance.^[21] However, particular attention has to be focused on the potential limits: it is fundamental to define the “safe” potential range where all materials present in the electrode can operate without degradation. In this context, the electrochemical stability window of AC in Li-salt containing electrolytes plays a crucial role.^[8] Indeed, the so called “safe potential window” or “capacitive potential region” of the high surface area carbon material drastically limits the use of these electrodes at potentials above 1.6–1.5 V vs. Li/Li⁺ in common electrolytes for Li-ion batteries (e.g. 1 M LiPF₆ in EC/DMC).^[8] The obvious hypothesis is that the enormous available area of the activated carbon accelerates the electrolyte decomposition, thus forming a solid electrolyte interphase (SEI) on the active material, blocking the micropores, increasing the resistance and allowing gas generation, with drastic consequences on the degradation of the electrode and of the entire cell. For this reason, the potential region below 1.5 V vs. Li/Li⁺ is not attractive and, so far, unexplored for activated carbon electrodes.

However, in literature is reported the use of AC as negative electrode either as pure active material or in a bi-material

[a] Dr. S. Dsoke
Helmholtz-Institute Ulm for Electrochemical Energy Storage (HIU)
P.O. Box 3640
D-76021 Karlsruhe, Germany
and
Institute for Applied Materials (IAM)
Karlsruhe Institute of Technology (KIT)
Hermann-von-Helmholtz-Platz 1
D-76344 Eggenstein-Leopoldshafen, Germany
E-mail: sonia.dsoke@kit.edu

composite electrode together with LTO.^[17,23–25] In such situation, due to the presence of AC, the lower potential cut-off should not cross the borderline of 1.5 V vs. Li/Li⁺. Nevertheless, when the cell runs at elevated currents it is unavoidable that the electrode reach potentials lower than this critical limit.^[26] In some scientific report composite electrodes based on AC and a battery-type material are even evaluated until the lower cut-off of 0 V vs. Li/Li⁺.^[27,28] Another work reports the use of a composite electrode based on AC and single-walled carbon nanotubes as negative electrode cycled between 3.5–0 V vs. Li/Li⁺.^[29] At this point, it is not clear which kind of degradation can happen on the AC surface and how this degradation can impact the device performance. In order to answer this question, a systematic study with (only) AC must be conducted in the low potential region. In this line, the aim of the present work is to evaluate the behavior of AC at potentials lower than 1.5 V vs. Li/Li⁺ and understand if there is any possibility to enlarge the cathodic working potential window in Li-salt containing electrolytes, without significant negative impact on resistance, stability and capacity.

2. Results and Discussion

2.1. Electrochemical Behavior of AC Electrodes in the Expanded Potential Range

Figure 1 displays consecutive cyclic voltammetry (CV) scans performed on an AC electrode. The first cycle (black curve)

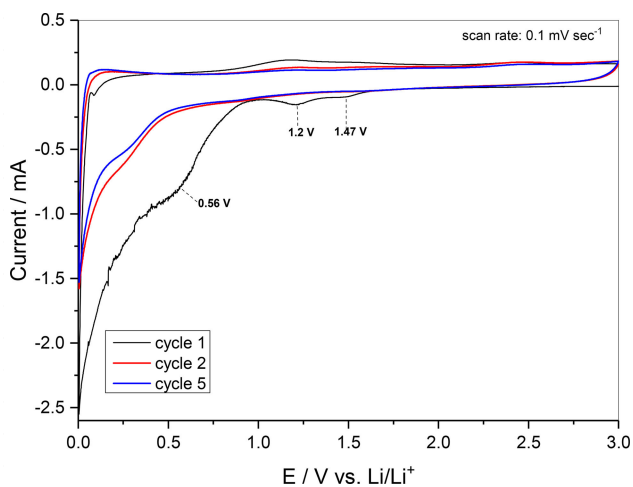


Figure 1. Cyclic voltammetry profiles of an AC electrode in the potential range 3.0–0.005 V vs. Li/Li⁺.

shows three reductive processes at 1.47 V, 1.2 V and 0.56 V vs. Li/Li⁺.

These processes can be attributed to the electrolyte decomposition on the AC surface with formation of an SEI and lithium insertion inside the micropores of the activated carbon, accompanied by possible interaction with the functional groups of the carbonaceous material.^[30,31] Most probably, it is not

possible to reversibly extract all lithium ions inserted during the first reduction step. However, in the subsequent cycles, a broad peak at low potential (between 0.4–0.005 V vs. Li/Li⁺) is still present, indicating a reversible faradaic phenomenon probably accompanied by Li-insertion and de-insertion in the remaining free micropores of the AC. Above 0.5 V vs. Li/Li⁺ the behavior is more capacitive, without any faradaic peaks, indicating that the AC partially maintains a certain double layer character.

In order to understand the impact of the lower potential limit on the reversible capacity, the irreversible capacity loss, the resistance and the cycling stability of AC, a set of identical electrodes were cycled between 3.0 V vs. Li/Li⁺ and different lower potential cut-offs. In detail, seven different potential ranges were evaluated with the same upper potential of 3.0 V and the lower potential of 1.5 V, 1.3 V, 1.0 V, 0.5 V, 0.2 V, 0.1 V and 0.005 V vs. Li/Li⁺, respectively. Small irreversibility (asymmetry in the reduction/oxidation curve) can be also observed on electrodes cycled down to 1.5 V, where it is supposed that only double layer charge storage mechanism is involved. However, after 10 cycles the profile shows the triangle shape typical for EDLCs (Figure 2 (a)). Below 1.5 V a change in slope in the first discharge profile, due to faradaic reactions, can be clearly observed (Figure 2 (b)). At potentials lower than 0.8 V the slope changes again (Figure 2 (c) and (d)).

Figure 3 reports the performance of AC electrodes, in terms of capacity and columbic efficiency, during the first 10 cycles at 0.1 Ag⁻¹. A clear trend can be recognized: the lower is the minimum potential cut-off, the higher the reversible capacity is (Figure 3 (d)). However, lowering the potential cut-off negatively affects the irreversible capacity loss at the first cycle, which reaches a value of c.a. 900 mAh g⁻¹ when the electrode is cycled between 3–0.01 V vs. Li/Li⁺ (Figure 3 (c)).

As expected, the rate capability (Figure 4) decreases with the increase of the potential span (by increasing the fraction of faradaic-type reaction). The highest rate capability can be reached by the electrode cycled between 3 and 1.5 V. In this case, AC maintains its capacitive behavior without any faradaic contribution. It is important to notice that the electrode cycled between 3.0 and 1.0 V has the worse rate capability among all electrodes and does not match the overall trend. This is a clear indication that at 1.0 V some drastic modification, which negatively affect the kinetics, occurs on the electrode surface. The bad electrode kinetics remains unchanged if the potential is not driven to lower values. This is a very critical point to be considered since in some publications the potential of electrodes containing AC is brought exactly to 1.0 V vs. Li/Li⁺.^[23,32]

2.2. Impedance Study During the First Three Cycles

In order to clarify the mechanism of SEI formation, the evolution of the resistance with the potential and to understand why the electrode cycled between 3.0–1.0 V has such anomalous behavior, electrochemical impedance spectroscopy (EIS) was conducted. EIS was performed at different potentials during the first reduction and oxidation scans. The most relevant changes on the Nyquist plot can be observed during

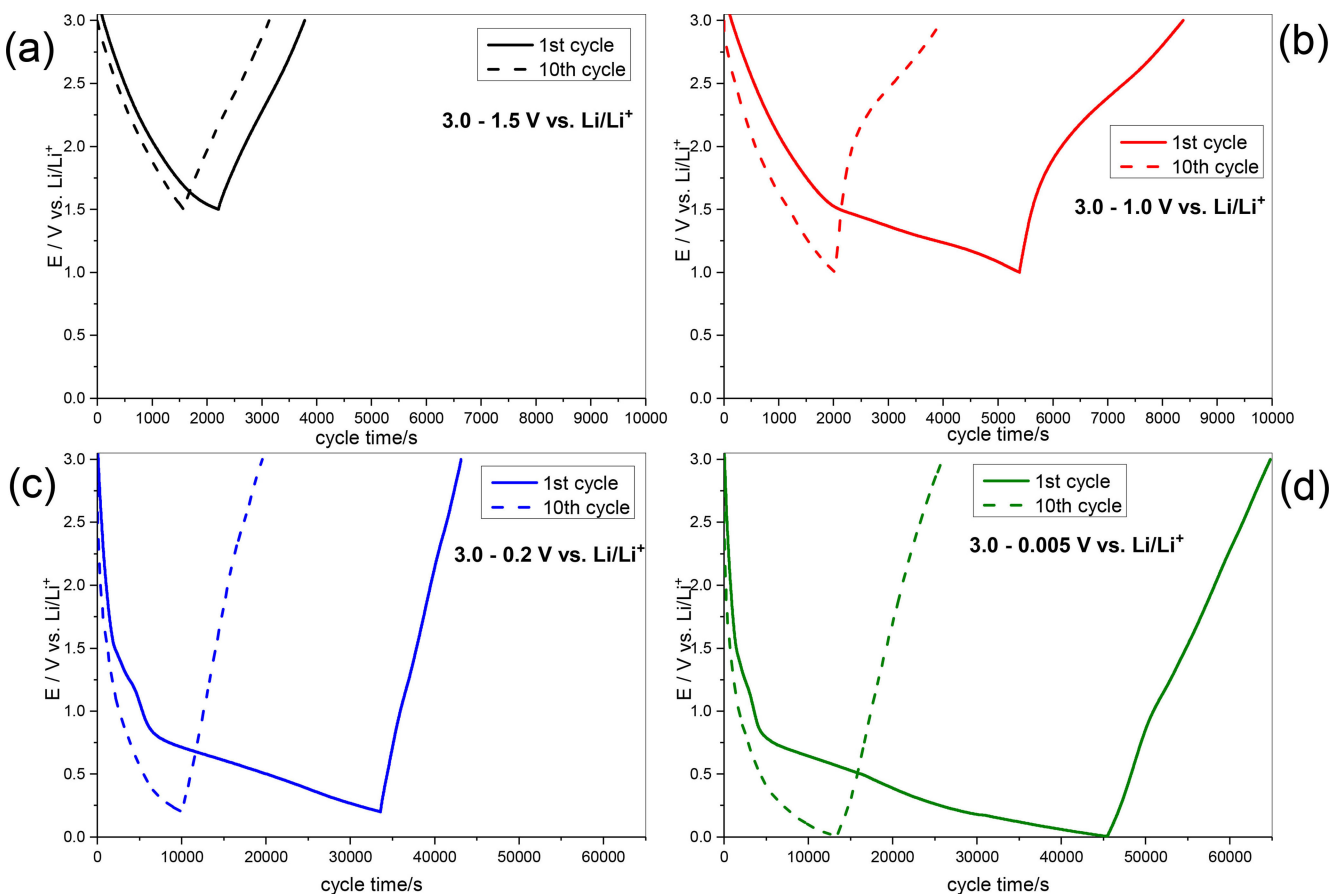


Figure 2. Comparison of 1st and 10th cycle profile of AC electrodes in different potential ranges at 0.1 A g^{-1} .

the first cathodic scan (Figure 5a). The fresh electrode shows the typical spectrum for EDLC, with a quasi-vertical line at the medium-low frequencies, indicating a double layer storage mechanism, and a semicircle at medium-high frequencies, which is mainly related to the contact resistance (R_{contact}). R_{contact} includes the contact between electrode and current collector and grain boundaries contact.^[33] From 3.0 V to 2.5 V the spectra do not change and the capacitive behavior is well retained. However, already at 2.0 V the slope of the low frequency line clearly changes. It is important to consider that, in Li-ion capacitors, 2.0 V is still considered a “safe” potential and, as already mentioned, the cathodic limit is generally about 1.5 V vs. Li/Li⁺.^[8] The deviation from the ideal capacitive behavior at low frequencies suggests that some irreversible process can occur also inside the so considered “safe” potential window. This deviation is an indication of a hindered penetrability of the ions inside the micro-pores of the activated carbon.^[34,35] It is recognized that for amorphous and highly porous carbons, the SEI starts to form at higher potential in comparison to graphitized carbons,^[36] which can explain this slight degradation already at that potential. The series of Nyquist plots recorded during the first cycle are reported in Figure 5 (a) and (b).

During the first cathodic scan, it is possible to observe a progressive increase of the size of the high frequency semicircle and a decrease of the slope at low frequencies. At this stage,

due to the presence of faradaic reactions, the high-frequency semicircle contains also the contribution of the charge transfer resistance (R_{CT}) and of the SEI film resistance (R_{SEI}). During the reverse scan (anodic) the diameter of the semicircle decreases and at low frequencies a mixed diffusive/capacitive behavior can be recognized. Anyway, when the system returns back to 3 V the spectra completely lose the typical characteristic for a capacitive-like behavior, which means that the process is irreversible. More information can be taken from the $\log[-Z''(W)]$ vs $\log(f)$ plot (Figure 5 (c) and (d)). This graphical representation provides a rich source of insights into the experimental system.^[37,38] The slopes at low frequency represent the constant phase element (CPE) fractional exponents (α). The CPE impedance is: $Z_{\text{CPE}} = Q^{-1}(jW)^{-\alpha}$, where Q is the CPE coefficient and $\alpha = 1$ for an ideal capacitor. Departure from 1 provides an indication of distributed processes. Figure 6 (a) resumes the slopes at low frequencies calculated from the $\log[-Z'']$ vs $\log(f)$ plots for the first three cycles. At OCV the value of α is 0.9, indicating a near capacitive behavior. Above 1.0 V the CPE exponent has values close to 0.7. After that, α quickly decreases until reaching, at very low potentials, values around 0.4–0.5, which are typical for diffusion behavior (i.e., Warburg-like). During the subsequent cycles, the α parameter has a value of around 0.7 for potentials between 3.0 and 1.0 V and decreases again at lower potentials in a reproducible way. This indicates that, after the first cycle, a mixed diffusive-capacitive

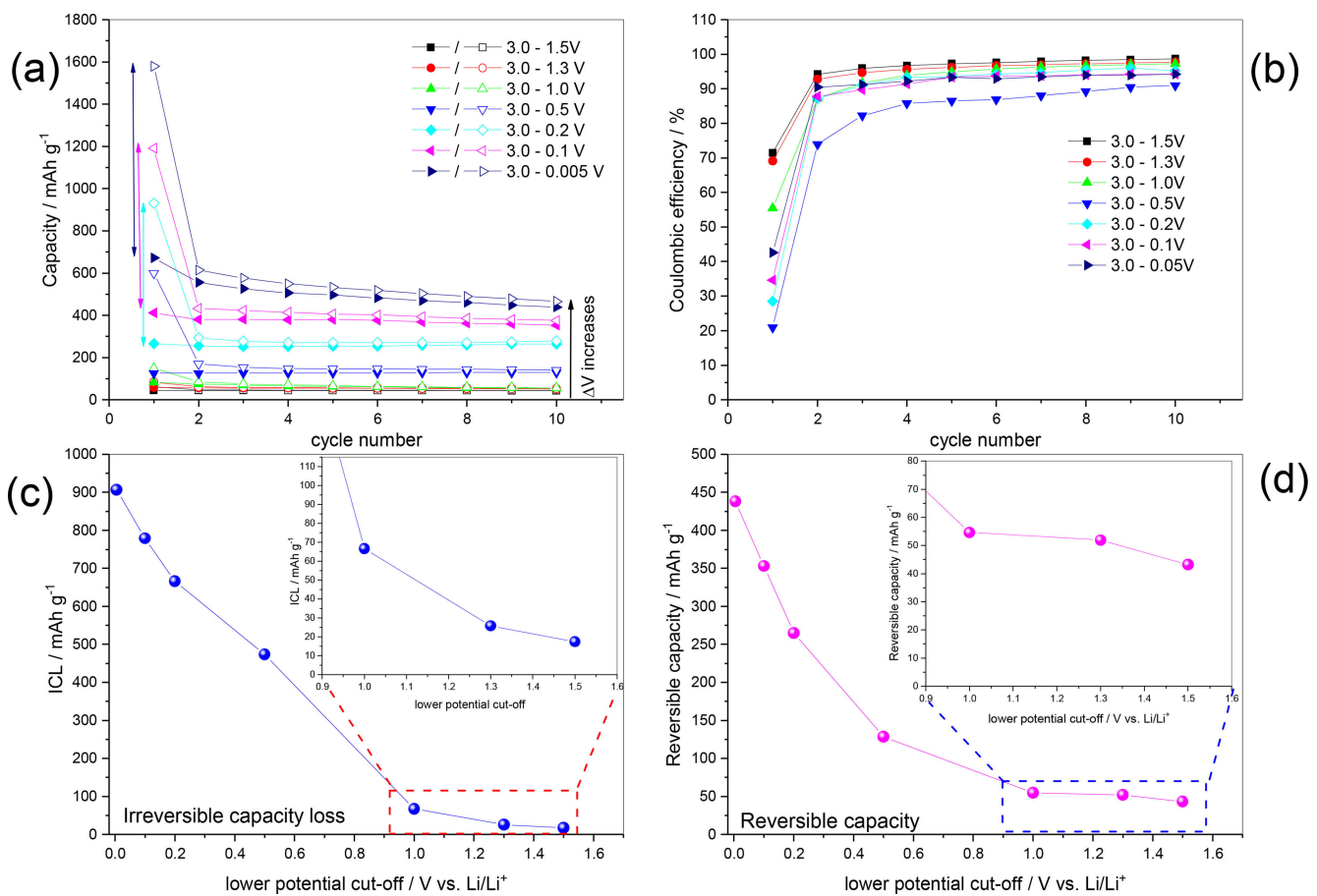


Figure 3. Values of a) capacities, b) columbic efficiency, c) irreversible capacity at the first cycle and d) reversible average capacity during the first 10 galvanostatic cycles of AC electrodes at 0.1 A g⁻¹.

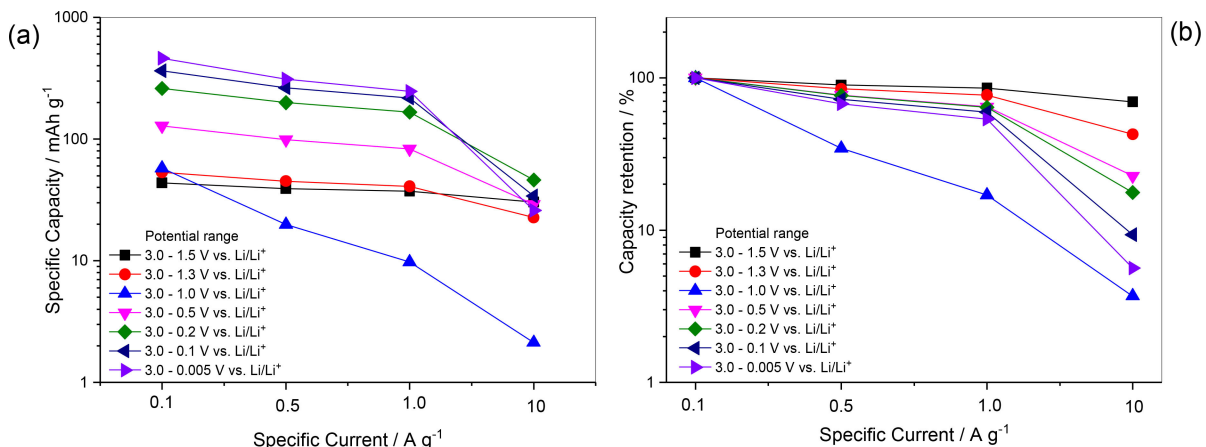


Figure 4. Rate capability of AC electrodes cycled in different potential ranges. Each value is the average of 5 consecutive cycles (the effect of initial irreversible capacity is excluded).

mechanism occurs between 3.0–1.0 V and a diffusion-like mechanism is dominant at lower potentials.

The frequency related to the maximum point of the high frequency semicircle is about 800 Hz on fresh electrodes. This value shifts to lower frequencies during the cathodic scan, reaching 420 Hz at 0.005 V, indicating that, as the electro-

chemical reduction proceeds, new processes with different time constants are raising and overlapping to the contact resistance. However, only one semicircle can be observed. This includes the R_{contact} , R_{SEI} and R_{CT} with their related capacitances. For this reason, only the total values of $R_{\text{contact} + \text{SEI} + \text{CT}}$ are considered in this study which are, for sake of simplicity, named as R_{HMF}

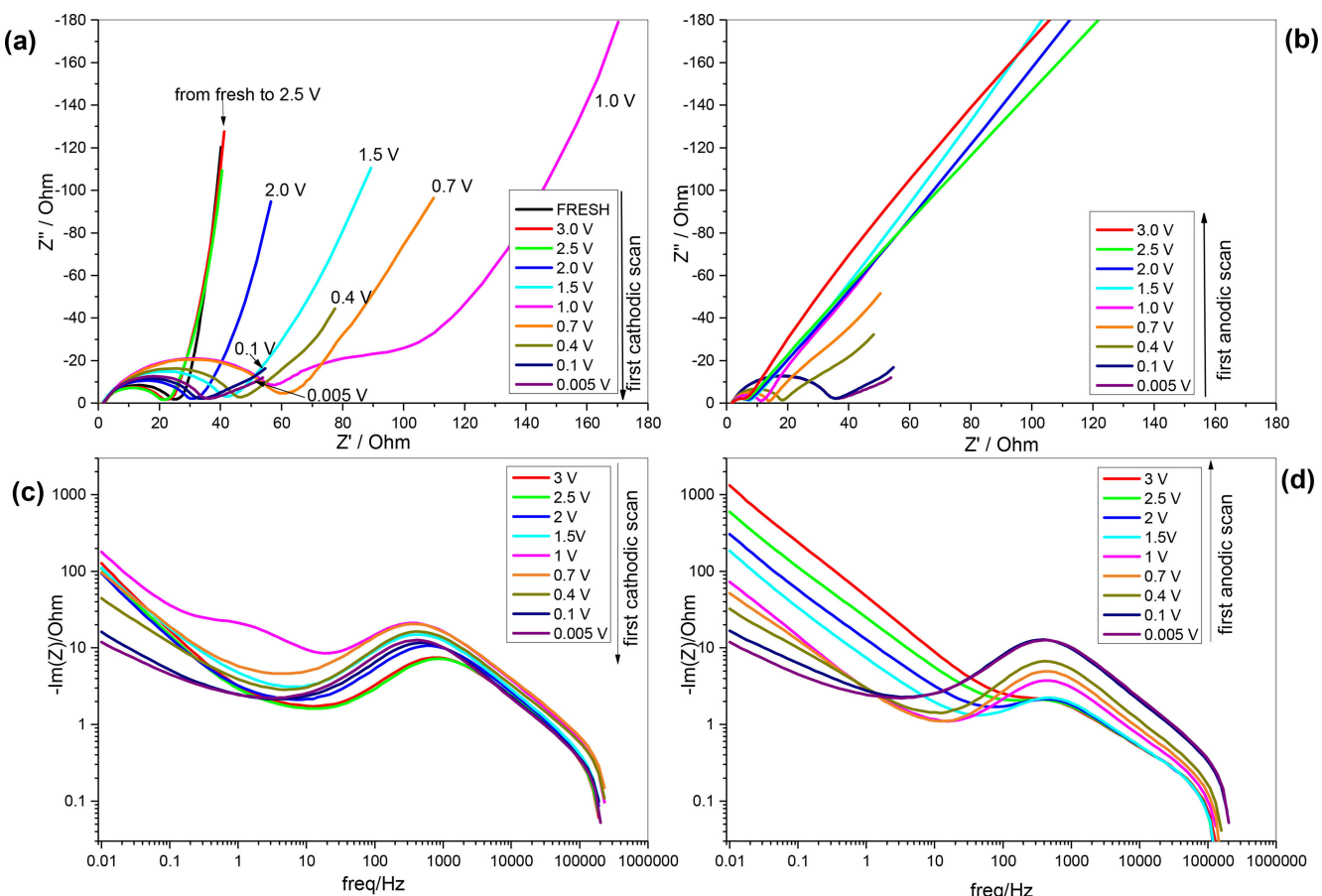


Figure 5. Nyquist plots of an AC electrode at different potentials during a) the first cathodic and b) first anodic scans. c) and d) imaginary part of complex plane vs. frequency plots.

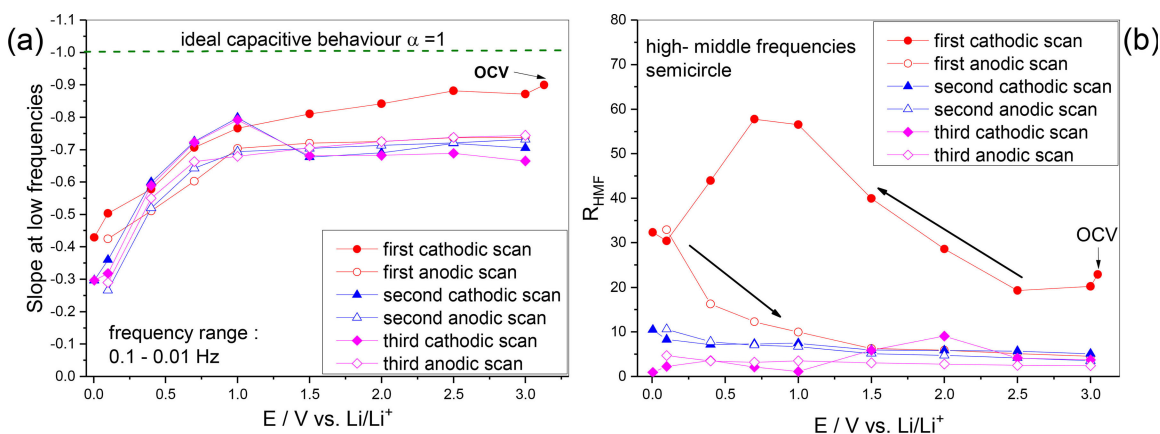


Figure 6. a) Slopes at low frequencies of the Imaginary vs. frequency plots and b) sum of contact, SEI and charge transfer resistances during the first three cycles.

(resistance related to the high-middle frequency semicircle). During the first reduction, the R_{HMF} increases as the potential reaches 1.0 V–0.7 V (Figure 6).

After that, it rapidly decreases until the end of the cathodic scan (0.005 V) to a value of c.a. 30 Ohm. As concerning the SEI formation, this behavior is in agreement with previous studies on other type of carbonaceous materials, which prove that the

SEI formed at high potential is more resistive in nature and it becomes more conductive at low potentials.^[35] During the first anodic scan, the resistance further decreases, reaching the value of 7 Ohm at 1.5 V, which indicates that the SEI is still modifying and becoming more conductive. After that, and in the subsequent two cycles, the R_{HMF} remains more or less unaltered with the potential.

2.3. Cycling Stability and Ageing Study of AC Electrodes Cycled in Various Potential Ranges

Cycling stability is a very important aspect for both supercapacitors and batteries. Herein, the influence of the lower potential cut-off on the stability was investigated by performing repeated charge/discharge cycles at the current of 1 A g^{-1} and analyzing the capacity retention and as well the resistances. When the electrode is cycled in the ranges 3.0–1.5 V and 3.0–1.3 V, where mainly only double layer mechanism is involved, the capacity is very stable with values around 40 mAh g^{-1} . In the potential range 3.0–1.0 V the performances drastically drop down, with a capacity of only 15 mAh g^{-1} . By further increasing the ΔV the capacity enhances, but the cycling stability decreases (Figure 7). The best compromise capacity/stability can be reached when the electrode is cycled in the potential range 3.0–0.5 V vs. Li/Li⁺. Impedance spectra were recorded at 3.0 V vs. Li/Li⁺ on fresh electrodes and on electrodes cycled 1000 times in the various potential ranges (Figure 8).

Obviously, the features of the spectra recorded on electrodes cycled with the lower cut-off of 1.5 and 1.3 V are similar to those of the fresh electrode. In these cases, no irreversible faradaic reactions occur and the spectra resemble to typical ones for EDLCs. In agreement with the spectra recorded during the first cycle at different potentials (Figure 5), also in this case the worse performance can be observed for the electrode cycled between 3.0–1.0 V. This result confirms, one more time, that the high resistance, probably due to the formation of non-conductive SEI and pore obstruction, is the main reason for the low capacity. In all other cases, the spectra show a similar behavior, with a semicircle at high-medium-frequencies and an inclined line at mid-low frequencies.

In Figure 8 it is possible to observe that, in the high to middle-frequency region, the Nyquist plots show differences in the bulk electrolyte resistance (R_{EL} , calculated by the intercept with the real axis) and in the size of the semicircle. In some case (especially on electrodes cycled at low potential), it is clearly possible to distinguish two semicircles, which represent the $R_{\text{contact+SEI}}$ and R_{CP} at high and medium frequencies, respectively.

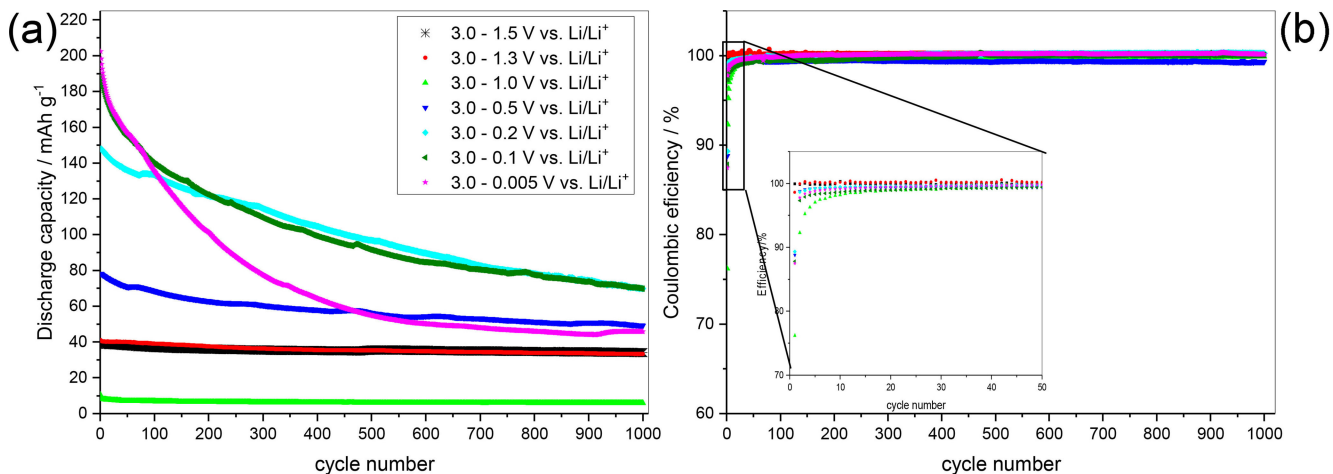


Figure 7. a) discharge capacities and b) columbic efficiency of AC electrodes cycled at 1 A g^{-1} and different potential ranges.

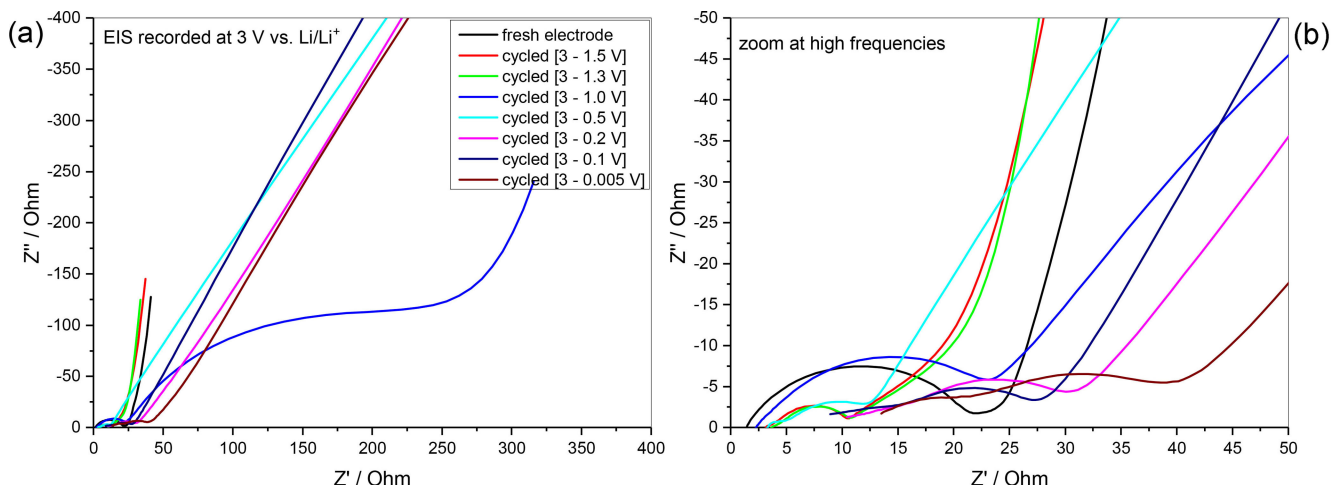


Figure 8. EIS of fresh and cycled AC electrodes recorded at 3 V vs. Li/Li⁺.

However, in other cases, the two semicircles are overlapped (Figure 8 (b)). In this study, the total resistance (R_{TOT}) has been compared and been defined as the sum R_{EL} , $R_{contact}$, R_{SEI} and R_{CT} . The values of R_{TOT} which is represented in Figure 9 (a), are between 10–50 Ohm, with the exception of the electrode cycled down to 1.0 V, which possesses a R_{TOT} of 280 Ohm. Overall, the electrodes cycled down to 1.5, 1.3 and 0.5 V vs. Li/Li⁺ display the lowest R_{TOT} with values of 10 Ohm. By decreasing the lower cut-off potential to 0.2 V and 0.1 V the resistance raises to 30 Ohm. Finally, the electrode cycled between 3.0–0.005 V shows a resistance of 50 Ohm. Figure 9 (b) reports the slopes calculated from the $\log[-Z'']$ vs $\log(f)$ plots in the low frequency region. Also in this case, the electrode cycled down to 1.0 V shows the worse behavior, with a α value of 0.43. On the other side, the electrodes cycled at lower potential cut-offs (0.5, 0.2, 0.1 and 0.005 V) still show a partial capacitive behavior when the electrode potential is returned back to 3 V vs. Li/Li⁺, with α values of about 0.75–0.8. By summing up these results, the choice of 0.5 V as lower potential cut-off, can be considered the best one in term of compromise stability-capacity-resistance.

3. Conclusions

Motivated by the necessity to expand the cathodic potential window of activated carbon electrodes, we explored the electrochemical performance of one commercial material in different potential windows, by lowering the potential until the limit of 0.005 V vs. Li/Li⁺. Activated carbon, which was previously never explored in such low potential window, can deliver relatively high capacity, similar to those of other carbonaceous materials for Li-ion batteries (like hard or soft carbons). The most important point to consider is the critical potential of 1.0 V vs. Li/Li⁺, which was already used as lower cut-off limit in some publication, when the activated carbon is part of a composite electrode together with a faradaic material.

Indeed, if the potential is limited to 1.0 V, the activated carbon completely loses its capacitor-type features, displaying a huge resistance and very low capacity. This can be due to the obstruction of the pores induced by the electrolyte decomposition and a different nature of the SEI, which is less conductive. On the other side, by pushing the potential to 0.5 V, the capacity increases and still some capacitive features are retained. At even lower potentials (0.2 V, 0.1 V and 0.005 V vs. Li/Li⁺) the gain in capacity is even higher, but the electrode shows worse performance in terms of rate capability, resistance and cycling stability. This study opens novel frontiers and perspectives on the use of an activated carbon at low potential. However, still a lot of work can be done, by for example, tuning the different properties of the carbon (like pore size, surface area and functional groups). Moreover, this work was based on the electrochemical understanding of this system. Additional analytical study on the electrode structure and surface chemistry, which can be done, for example, by performing XPS analysis on electrodes cycled in different potential ranges can give further insights and direction for designing novel materials for energy storage systems.

Experimental Section

Electrode Preparation

A commercial activated carbon (Haycarb PLC) which was extensively characterized in previous works^[6,38] was employed as active material for electrode preparation. This activated carbon has a BET surface area of 1705 m² g⁻¹ and a meso- and micropore volumes of 0.281 and 0.646 m³ g⁻¹, respectively. The average pore diameter is about 1.2 nm [6]. The working electrodes were prepared by mixing activated carbon as active material and SuperP (Imerys, earlier Timcal) as conductive additive with a binder solution in the following way: (i) PVDF binder (Solvay) was firstly dissolved in NMP (Sigma Aldrich), (ii) activated carbon and SuperP were then successively added to the binder solution. The final slurries were coated onto the Cu foil using doctor blade technique with a wet thickness of 100 µm. The cast layers were dried first for 2 h at 60°C

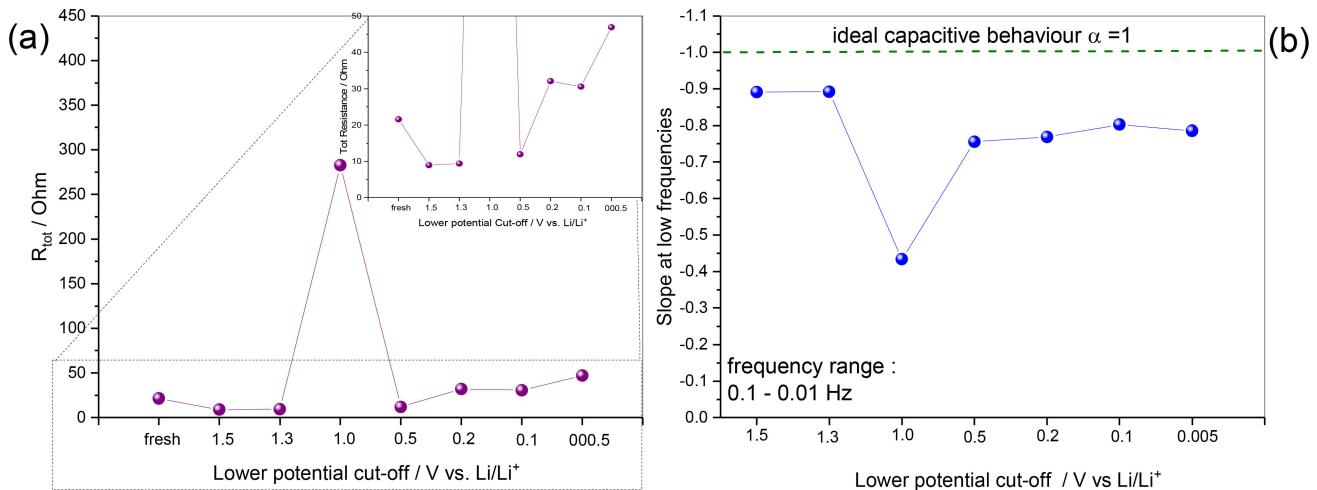


Figure 9. a) values of total resistances and of b) the low frequency slope of AC electrodes cycled in different potential ranges, as calculated from the EIS of Figure 8.

and then at 80 °C for 10 h to remove any residual solvent. Circular electrodes (with 12 mm diameter) were punched out from the layer and pressed at 7 tons with a hydraulic laboratory press. The final electrodes have a thickness of 40 µm ± 5 and a mass loading of 1.8 mg ± 0.2. The electrodes were finally dried at 120 °C under vacuum for 12 hours in order to remove traces of water.

Cell Assembly

Swagelok® type cells have been used for all electrochemical experiments. AC electrodes were used as working electrodes, metallic lithium as counter and reference electrode. Positive and negative electrodes were separated by three glass microfiber filter separators (Whatman® GF/A, Aldrich). All electrochemical experiments were conducted in 1 M LiPF₆ in EC:DMC (1:1 wt%) electrolyte (BASF).

Electrochemical Characterization

Five subsequent cyclic voltammetry were carried out with a scan rate of 0.1 mV sec⁻¹ in a voltage range 3.0–0.05 V vs. Li/Li⁺. Galvanostatic Cycling with Potential Limitation (GCPL) was carried out at various specific currents ranging from 0.1 to 10 A g⁻¹ (10 cycles for each current) with different lower potential cut-offs. Long term cycling tests (i.e., 1000 cycles) were performed at 1 A g⁻¹. Electrochemical Impedance Spectroscopy (EIS) measurements were performed by applying a low amplitude alternating voltage of 5 mV at different bias voltages between 3.0 and 0.05 V vs. Li/Li⁺ during the first three charge and discharge cycles and as well on fresh and cycled cells to evaluate the effect of long term cycling. The frequency was set in a range from 500 kHz to 10 mHz. All electrochemical measurements were conducted at 25 °C with a VMP3 multi-channel potentiostat/galvanostat (Bio-logic Science Instrument, France), equipped with an EC-Lab® software.

Acknowledgements

The author gratefully acknowledges the financial support of the Ministry of Science, Research and Art (MWK) Baden-Württemberg through the Brigitte-Schlieben-Lange-Programm. This work contributes to the research performed at CELEST (Center for Electrochemical Energy Storage Ulm-Karlsruhe).

Conflict of Interest

The authors declare no conflict of interest.

Keywords: activated carbon • intercalations • lithium-ion capacitor • potential window expansion • SEI formation

- [1] L. L. Zhang, X. S. Zhao, *Chem. Soc. Rev.* **2009**, *38*, 2520–253.
- [2] M. Inagakia, H. Konnoa, O. Tanaike, *J. Power Sources* **2010**, *195*, 7880–7903.

- [3] Z. Peng, Z. Guo, W. Chu, M. Wei, *RSC Adv.* **2016**, *6*, 42019–42028.
- [4] W. Qiao, S.-Ho Yoon, I. Mochida, *Energ. Fuel.* **2006**, *20*, 1680–1684.
- [5] P. Sharma, T. S. Bhatti, *Energ. Convers. Manage.* **2010**, *51*, 2901–2912.
- [6] A. González, E. Goikolea, J. Andoni Barrena, R. Mysyk, *Renewable Sustainable Energy Rev.* **2016**, *58*, 1189–1206.
- [7] S. Phadke, S. Amara, M. Anouti, *ChemPhysChem* **2017**, *18*, 2364–2373.
- [8] T. Zhang, B. Fuchs, M. Secchiaroli, M. Wohlfahrt-Mehrens, S. Dsoke, *Electrochim. Acta* **2016**, *218*, 163.
- [9] G. G. Amatucci, F. Badway, A. Du Pasquier, T. Zheng, *J. Electrochem. Soc.* **2001**, *148*, A930–A939.
- [10] K. Naoi, S. Ishimoto, J. Miyamoto, W. Naoi, *Energy Environ. Sci.* **2012**, *5*, 9363.
- [11] J. Ding, W. Hu, E. Paek, D. Mitlin, *Chem. Rev.* **2018**, *118*, 6457–6498.
- [12] S. R. Sivakkumar, A. G. Pandolfo, *Electrochim. Acta* **2012**, *65*, 280–287.
- [13] V. Aravindan, J. Gnanaraj, Y.-S. Lee, S. Madhavi, *Chem. Rev.* **2014**, *114*, 11619–11635.
- [14] J. J. Ren, L. W. Su, X. Qin, M. Yang, J. P. Wei, Z. Zhou, P. W. Shen, *J. Power Sources* **2014**, *264*, 108–113.
- [15] W. J. Cao, J. P. Zheng, *J. Power Sources* **2012**, *213*, 180–185.
- [16] X. Zhang, R.-S. Kühnel, M. Schroeder, A. Balducci, *J. Mater. Chem. A* **2014**, *2*, 17906–17913.
- [17] M. Secchiaroli, G. Giuli, B. Fuchs, R. Marassi, M. Wohlfahrt-Mehrens, S. Dsoke, *J. Mater. Chem. A* **2015**, *3*, 11807–11816.
- [18] N. Böckenfeld, A. Balducci, *J. Power Sources* **2013**, *235*, 265.
- [19] N. Böckenfeld, R.-S. Kühnel, S. Passerini, M. Winter, A. Balducci, *J. Power Sources* **2011**, *196*, 4136–4142.
- [20] S.-B. Ma, K.-W. Nam, W.-S. Yoon, X.-Q. Yang, K.-Y. Ahn, K.-H. Oh, K.-B. Kim, *Electrochim. Commun.* **2007**, *9*, 2807–2811.
- [21] M. Secchiaroli, R. Marassi, M. Wohlfahrt-Mehrens, S. Dsoke, *Electrochim. Acta* **2016**, *219*, 425–434.
- [22] D. Cericola, R. Kötz, *Electrochim. Acta* **2012**, *72*, 1–17.
- [23] D. Cericola, P. Novák, A. Wokaun, R. Kötz, *J. Power Sources* **2011**, *196*, 10305–10313.
- [24] E. Zhao, C. Qin, H.-R. Jung, G. Berdichevsky, A. Nese, S. Marder, G. Yushin, *ACS Nano* **2016**, *10*, 3977–3984.
- [25] H.-S. Choi, J. H. Im, T. H. Kim, J. H. Park, C. R. Park, *J. Mater. Chem.* **2012**, *22*, 16986.
- [26] S. Dsoke, B. Fuchs, E. Gucciardi, M. Wohlfahrt-Mehrens, *J. Power Sources* **2015**, *282*, 385–393.
- [27] J.-J. Yang, H.-I. Ki, Y.-J. Yuk, H.-J. Kim, S.-G. Park, *J. Electrochem. Soc. Te.* **2010**, *1*, 63–68.
- [28] H. I. Kim, J. J. Yang, H. J. Kim, S. G. Park, *ECS Trans.* **2008**, *16*, 185–190.
- [29] M. A. Azam, N. H. Jantan, N. Dorah, R. N. A. R. Seman, N. S. A. Manaf, T. I. T. Kudin, M. Z. A. Yahy, *Mat. Res. Bull.* **2015**, *69*, 20–23.
- [30] J. Zhang, X. Liu, J. Wang, J. Shi, Z. Shi, *Electrochim. Acta* **2016**, *187*, 134–142.
- [31] C. W. Park, S.-H. Yoon, S. I. Lee, S. M. Oh, *Carbon* **2000**, *38*, 995–1001.
- [32] V. Khomenko, E. Raymundo-Pinero, F. Béguin, *J. Power Sources* **2008**, *177*, 643–651.
- [33] S. Dsoke, X. Tian, C. Täubert, S. Schlüter, M. Wohlfahrt-Mehrens, *J. Power Sources* **2013**, *238*, 422–429.
- [34] L. Permann, M. Lätt, J. Leis, M. Arulepp, *Electrochim. Acta* **2006**, *51*, 1274–1281.
- [35] H.-K. Song, J.-H. Sung, Y.-H. Jung, K.-H. Lee, L. H. Dao, M.-H. Kim, H.-N. Kim, *J. Electrochim. Soc.* **2004**, *151*, E102–E109.
- [36] C. A. Bridges, X.-G. Sun, J. Zhao, M. P. Paranthaman, S. Dai, *J. Phys. Chem. C* **2012**, *116*, 7701–7711.
- [37] A. Laheääär, A. Jänes, E. Lust, *Electrochim. Acta* **2011**, *56*, 9048–9055.
- [38] A. Laheääär, H. Kurig, A. Jänes, E. Lust, *Electrochim. Acta* **2009**, *54*, 4587–4594.
- [39] H. Y. Tran, M. Wohlfahrt-Mehrens, S. Dsoke, *J. Power Sources* **2017**, *342*, 301–312.

Manuscript received: August 27, 2018
Accepted Article published: September 27, 2018
Version of record online: October 18, 2018